Studia Universitatis "Vasile Goldiş", Seria Ştiinţele Vieţii
Vol. 28 issue 4, 2018, pp. 159-166

INUNDATION AREA INVESTIGATION APPROACH USING REMOTE SENSING TECHNOLOGY ON 2017 FLOODING IN SAKON NAKHON PROVINCE THAILAND

Tanutdech Rotjanakusol[1,2], Teerawong Laosuwan[1,2]*
[1]Department of Physics, Faculty Science, Mahasarakham University, Khamriang, Kantarawichai, Mahasarakham, 44150, Thailand.
[2]Space Technology and Geoinformatics Research Unit, Faculty of Science, Mahasarakham University, Mahasarakham, 44150 Thailand

Abstract: Flooding is a natural phenomenon occurring frequently in different areas of Thailand. In July 2017, it rained unceasingly in Sakon Nakhon owing to the influence of SONCA, a tropical storm. Flooding affected the livelihoods of local inhabitants and caused severe damage to agricultural areas. This study aimed to explore the inundation area, examination approach suitable for the regional level, particularly in the north-eastern part of Thailand. Flooding in Sakon Nakhon that occurred in 2017 was used as a case study. For implementation, data from Terra/Modis was analyzed along with the use of the 4 designed physical models comprising 1) the normalized difference vegetation index (NDVI), 2) the normalized difference water index (NDWI), 3) the modification of normalized difference water index (MNDWI), and 4) the desert flood index (DFI). The findings from these models were exploited for the ground surveys and accuracy assessment by Kappa statistics. It was found that analysis of the data from Terra/Modis and the use of DFI was the best approach. The overall accuracy = 94.44% and Kappa statistics = 0.9102. This implied that the approach in the study could identify the patterns of inundation areas efficiently.

Keywords: Remote sensing, flooding, NDVI, NDWI, MNDWI, DFI

INTRODUCTION

Natural disasters and severe natural phenomena cause humans to be unable to live their lives normally. They also cause significant damage to life as well as property, leading to social deterioration (Krausmann and Mushtaq, 2008; Brunda and Nyamathi, 2015). One of the most frequent disasters is flooding (41.4%), followed by earthquakes and storms. Asia is the most affected continent (Milly *et al*., 2002). For Thailand, the cost of damage from flooding has increased from 6,000 million baht in 1990 up to 40,000 million baht in 2000 and 1.44 trillion baht in 2011(Department of Disaster Prevention and Mitigation, 2013). In 2017, flooding in Thailand was regarded as the fourth worst devastation in the world after Japan's earthquake and tsunami in 2011, Japan earthquake in 1995, and Hurricane Katrina in the US in 2005 (Asian Disaster Reduction Center, 2012).

In the past, every region of Thailand had to face flooding issues annually on account of the geographic factors which place the country in a tropical zone of the peninsula. Its location is the main reason why Thailand is unable to avoid the influence of year round monsoons and storms (Thai Meteorological Department, 2017). Based on this information, there is an urgent indispensable requirement for damage and flood severity level assessment to provide information or a map displaying the scope of disaster areas (Amini, 2010; Kia *et al*., 2012; Saini and Kaushik, 2012; Blanc *et al*., 2012; Kim *et al*., 2014; Elkhrachy, 2015). A traditional approach like inundation mapping by ground survey involves high cost and significant time investment. Also, some areas are spacious and difficult to access. Remote sensing technology based on data from satellites, which can record incidents on earth and reflect electromagnetic waves to the sensors on the satellites (Uttaruk and Laosuwan, 2016; Laosuwan and Uttaruk, 2016; Rotjanakusol and Laosuwan, 2018; Uttaruk and Laosuwan, 2018), is applied along with physical models for flood damage assessment. The data from these satellites perfectly covers spacious areas that are otherwise difficult to access. It also involves less cost when compared to ground surveys (Gates, 1980; Gao, 1996; McFeeters, 1996; Xu, 2006; Wang, 2007; Singh and Singh, 2017)

In July 2017, it rained unceasingly in Sakon Nakhon, which is an area located in the northeastern part of Thailand, owing to the influence of SONCA (a tropical storm named so by Vietnam). As a result, disastrous flooding occurred and affected the livelihoods of local inhabitants. It also caused severe damage to agricultural areas. This study aimed to explore the inundation area, examination approach suitable for the regional level, particularly in the northeastern part of Thailand. The flooding in Sakon Nakhon in 2017 was used as a case study.

STUDY AREA AND DATA

Study area

Sakon Nakhon (Fig.1) is 1 of 20 north-eastern provinces in Thailand. It is located around latitude 16^o 45' to 18^o 15' N and longitude 103^o 15' to 104^o 30' E, covering the entire area of 9,605.76 km^2, around 172 m higher than sea level. Throughout the year, the temperature is around 26.20 ^{o}C, while average rainfall is between 1300 -2000 mm. Sakon Nakhon adjoins the following provinces: 1) Nong Khai to the north, 2) Nakhon Phanom to the east, 3) Kalasin and Mokdahan to the south and 4) Udon Thani to the west

Correspondence: Teerawong Laosuwan, Department of Physics, Faculty Science, Mahasarakham University, Khamriang, Kantarawichai, Maha Sarakham, 44150, Thailand, Tel/Fax. +66 4375 4379, email: teerawong@msu.ac.th

Data

Data from MODIS/Terra Satellite: The study relied on data from Terra/Modis (MOD09A1 V6 product) covering Sakon Nakhon, the study area (H27, V7). The MOD09A1 V6 product comprised the data in the form of 8-day surface reflectance composites with 500 m. pixels recorded in 7 bands (Table 1). The researcher downloaded the data from LAADS DAAC (https://ladsweb. modaps.eosdis.nasa.gov/).

Rainfall Data

In this study, we collected data for average monthly rainfall as measured from 21 rainfall stations covering the Sakon Nakhon region.

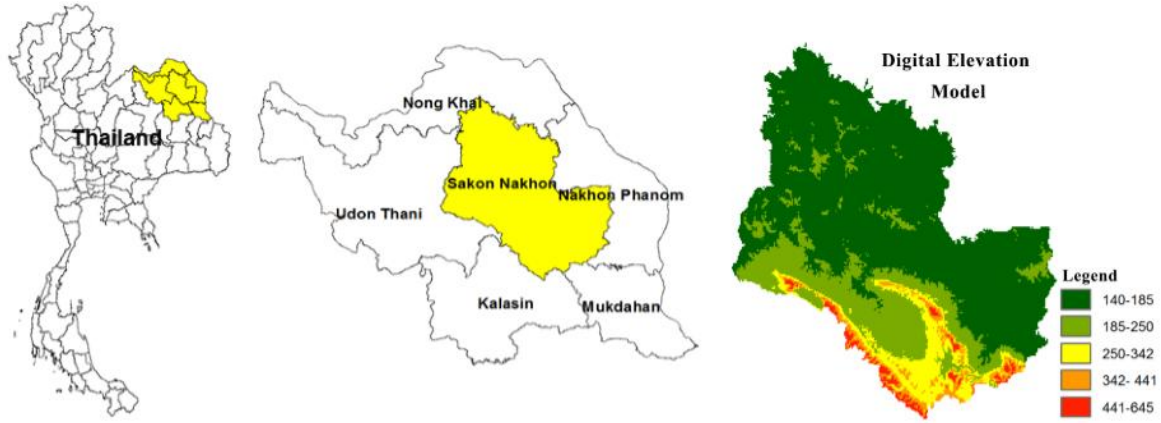

Fig. 1. Sakon Nakhon province

Tab. 1.

MOD09A1 Data Set

No. Band	Band Width (nm)	Band Name	Resolution
Band 1	620-670	RED	500m
Band 2	841-876	NEAR INFRARED	500m
Band 3	459-479	BLUE	500m
Band 4	545-565	GREEN	500m
Band 5	1230-1250	NEAR INFRARED	500m
Band 6	1628-1652	SORTHWAVE NFRARED	500m
Band 7	2105-2155	SORTHWAVE NFRARED	500m

METHODOLOGY

This section is shown in Fig. 2 with the following details.

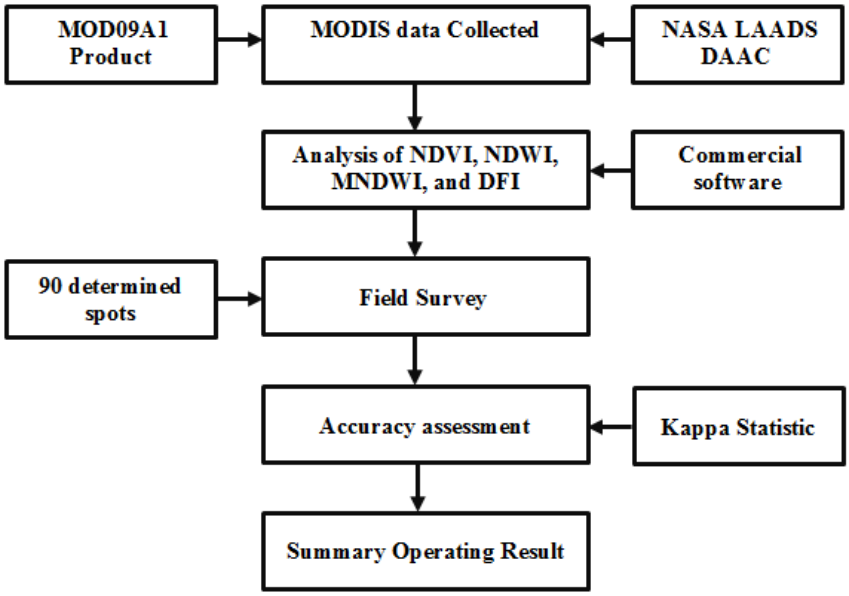

Fig. 2. Flowchart of the study

Studia Universitatis "Vasile Goldiş", Seria Ştiinţele Vieţii
Vol. 28 issue 4, 2018, pp. 159-166

Data Preparation

We used data from the satellite in 3 phases, namely pre-flooding, flooding phase, and post-flooding. Because the downloaded data from MOD09A1 V6 product was in the form of sinusoidal projection, the data had to be re-projected into WGS84/UTM zone 47 N before analysis.

Data Analysis

The study mainly focused on the 4 designed physical models, including NDVI by Rouse *et al*. (1973), NDWI by McFeeters (1996), MNDWI by Xu (2006), and DFI by Wang (2007). Theoretically, NDVI would fall between -1 to +1. If NDVI was close to +1, it represented dense green vegetation. However, it represented water areas if close to -1. Likewise, NDWI, MNDWI, and DFI would fall between -1 to +1, but with opposite results to NDVI. To clarify, it represented water areas if NDWI was close to +1. If it was close to -, it represented dense green vegetation. Table 2 describes the details for the equations of all 4 physical models previously mentioned. Next, we took the findings of analysis for the models of the ground surveys at 90 determined spots within the study area. The final step was accuracy assessment using Kappa statistics.

Tab. 2.

The details of 4 designed physical models

Physical models	Equation	References
NDVI	$NDVI = \frac{NIR - RED}{NIR + RED}$	17
NDWI	$NDWI = \frac{NIR - SWIR}{NIR + SWIR}$	19
MNDWI	$MNDWI = \frac{Green - SWIR}{Green + SWIR}$	20
DFI	$DFI = \frac{Green - SWIR + 0.1}{(Green + SWIR)(NDVI + 0.5)}$	21

RESULTS AND DISCUSSION

Findings of Data Analysis

Finding of Data Analysis by NDVI

The findings of data analysis by NDVI in all 3 phases indicated that pre-flooding possessed min = 0.128, max = 0.824, and std = 0.084. The flooding phase possessed min = -0.316, max = 0.853, and std = 0.16. The post-flooding possessed min = -0.037, max = 0.702, and std = 0.057. To make it easy for spatial analysis, the findings of data analysis by NDVI were separated into 5 ranges, i.e. -1.000 to -0.600, -0.600 to -0.200, -0.200 to 0.200, 0.200 to 0.600, and 0.600 to 1.000. The spatial analysis is shown in Fig. 3, from which the flooding phase apparently illustrated that the areas in the ranges of -1.000 to -0.600, -0.600 to -0.200, and -0.200 to 0.200 tended to increase in percentage due to flooding.

When these findings were compared with the rainfall, pre-flooding (May 2017) was with the rainfall = 301.100 mm and the mean of NDVI = 0.503. The flooding phase (July 2017) was with the rainfall = 796.500 mm and the mean of NDVI = 0.427. Post-flooding (September 2017) was with the rainfall = 796.500 mm and the mean of NDVI = 0.437. This meant that the more the rainfall increased, the higher the means of NDVI followed (dense vegetation). In contrast, the more the rainfall decreased, the lower the means of NDVI followed (little vegetation). In this study, it was found that the NDVI declined during floods due to flooding in the study area. The results of the 3 phases operation can be shown in Table 3.

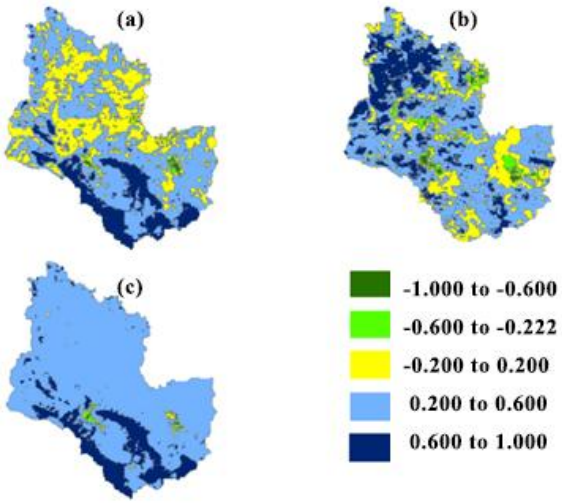

Fig. 3. NDVI (a) pre-flooding, (b) flooding phase, and (c) post-flooding

Tab. 3.

The results of 3 phases operation

Phases	Rainfall	NDVI (means)
Pre-flooding (May 2017)	301.100	0.503
Flooding phase (July 2017)	796.500	0.327
Post-flooding (September 2017)	203.400	0.437

Finding of Data Analysis by NDWI

The findings of data analysis by NDWI in all 3 phases indicated that pre-flooding possessed min = -0.827, max = 0.031, and std = 0.099. The flooding phase possessed min = 0.474, max = 0.852, and std = 0.142. Post-flooding possessed min = 0.234, max = 0.954, and std = 0.132. To make it easy for spatial analysis, the findings of data analysis by NDWI were separated into 5 ranges similar to NDVI. The spatial analysis is shown in Fig. 4, from which the flooding phase apparently illustrated that the areas in the ranges of -1.200 to -0.200, -0.200 to -0.600, and -0.600 to 1.000 tended to increase in percentage due to flooding.

When these findings were compared with the rainfall, pre-flooding (May 2017) was with the rainfall = 301.100 mm and the mean of NDWI = 0.427. The flooding phase (July 2017) was with the rainfall = 796.500 mm and the mean of NDWI = 0.523. Post-flooding (September 2017) was with the rainfall = 203.400 mm and the mean of NDWI = 0.337. This meant the more the rainfall increased, the higher the means of NDWI followed (more water area). In contrast, the more the rainfall decreased, the lower the means of NDWI followed (less water area). The results of the 3 phases operation can be shown in Table 4.

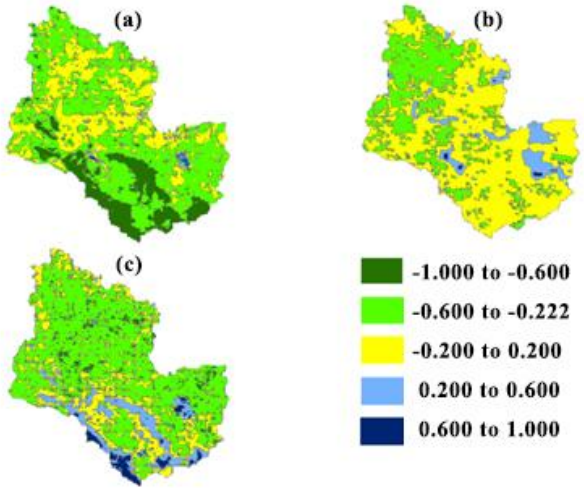

Fig. 4. NDWI (a) pre-flooding, (b) flooding phase, and (c) post-flooding

Studia Universitatis "Vasile Goldiş", Seria Ştiinţele Vieţii
Vol. 28 issue 4, 2018, pp. 159-166

Tab. 4.

The results of 3 phases operation

Phases	Rainfall	NDWI (means)
Pre-flooding (May 2017)	301.100	0.427
Flooding phase (July 2017)	796.500	0.523
Post-flooding (September 2017)	203.400	0.337

Finding of Data Analysis by MNDWI

The findings of data analysis by MNDWI in all 3 phases indicated that pre-flooding possessed min = -0.520, max = 0.983, and std = 0.153. The flooding phase possessed min = -0.357, max = 0.809, and std = 0.146. Post-flooding possessed min = -0.379, max = 1.027, and std = 0.191. To make it easy for spatial analysis, the findings of data analysis by MNDWI were separated into 5 ranges like NDVI and NDWI. The spatial analysis is shown in Fig. 5, from which the flooding phase apparently illustrated that the areas in the ranges of -0.200 to -0.200, -0.200 to -0.600, and -0.600 to 1.000 tended to increase in percentage due to flooding, similar to NDWI.

When these findings were compared with the rainfall, pre-flooding (May 2017) was with the rainfall = 301.100 mm and the mean of MNDWI = -0.522. The flooding phase (July 2017) was with the rainfall = 796.500 mm and the mean of MNDWI = 0.495. Post-flooding (September 2017) was with the rainfall = 203.400 mm and the mean of MNDWI = 0.130. This meant the more the rainfall increased, the higher the means of MNDWI followed (more water area). In contrast, the more the rainfall decreased, the lower the means of MNDWI followed (less water area). The results of the 3 phases operation can be shown in Table 5.

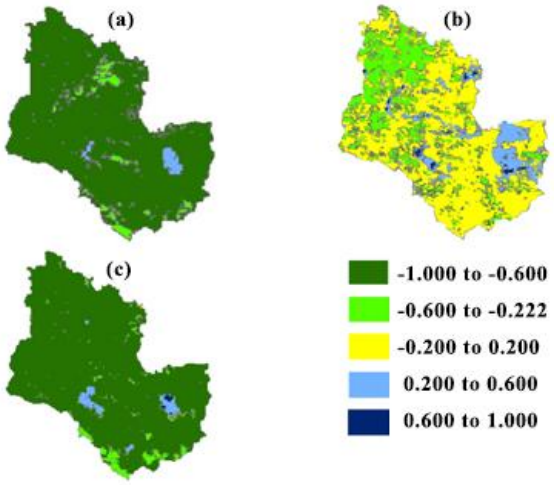

Fig. 5. MNDWI (a) pre-flooding, (b) flooding phase, and (c) post-flooding

Tab. 5.

The results of 3 phases operation

Phases	Rainfall	MNDWI (means)
Pre-flooding (May 2017)	301.100	-0.522
Flooding phase (July 2017)	796.500	0.495
Post-flooding (September 2017)	203.400	0.130

Finding of Data Analysis by DFI

The findings of data analysis by DFI in all 3 phases indicated that pre-flooding possessed min = -0.289, max = 0.296, and std = 0.030. The flooding phase possessed min = -1.009, max = 0.809, and std = 0.146. Post-flooding possessed min = -1.077, max = 0.941, and std = 0.146. To make it easy for spatial analysis, the findings of data analysis by DFI were separated into 5 ranges like NDVI, NDWI, and MNDWI. The spatial analysis is shown in Fig. 6, from which the flooding phase apparently illustrated that the areas in the ranges of -0.200 to -0.200, -0.200 to -0.600, and -0.600 to 1.000 tended to increase in percentage due to flooding, similar to NDWI and MNDWI.

When these findings were compared with the rainfall, pre-flooding (May 2017) was with the rainfall = 301.100 mm and the mean of DFI = 0.149. The flooding phase (July 2017) was with the rainfall = 796.500 mm and the mean of DFI = 0.700. Post-flooding (September 2017) was with the rainfall = 203.400 mm and the mean of DFI = 0.110. This meant the more the rainfall increased, the higher the means of DFI followed (more water area). In contrast, the more the rainfall decreased, the lower the means of DFI followed (less water area). The results of the 3 phases operation can be shown in Table 6.

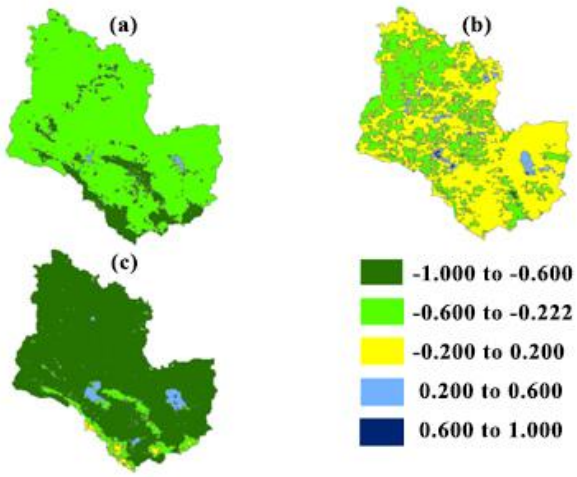

Fig. 6. DFI (a) pre-flooding, (b) flooding phase, and (c) post-flooding

Tab. 6.

The results of 3 phases operation

Phases	Rainfall	DFI (means)
Pre-flooding (May 2017)	301.100	0.149
Flooding phase (July 2017)	796.500	0.700
Post-flooding (September 2017)	203.400	0.110

Findings of Field Survey and Accuracy Assessment

With respect to the findings of accuracy assessment in this study, we concentrated on the classification of water areas and land in particular. The findings of the 4 physical models, comprising NDVI, NDWI, MNDWI, and DFI from 190 sample points (the ground survey points), were interpreted as follows: 1) The NDVI model possessed overall accuracy = 92.22% and Kappa statistics = 0.8883. 2) The NDWI model possessed overall accuracy = 93.33% and Kappa statistics = 0.8736. 3) The MNDWI model possessed overall accuracy = 93.33% and Kappa statistics = 0.8923, while the DFI model possessed overall accuracy = 94.44 % and Kappa statistics = 0.9102. When looking into the overall accuracy and Kappa statistics of the 4 physical models, DFI was found to have highest percentage for analysis accuracy. Fig. 7 describes the spatial data in the pre-flooding, flooding phase, and post-flooding by DFI.

According to Fig.7, it was discovered that there was land at 94.197 %, or 9,048.294 km^2, and water areas at 5.803 %, or 557.470 km^2 in the pre-flooding phase. In the flooding phase, there was land at 34.580 %, or 3,321.652 km^2, and water areas at 65.420 %, or 6,284.112 km^2. In post-flooding, there was land at 96.155 %, or 9,236.399 km^2, and water areas at 3.845 %, or 369.366 km^2.

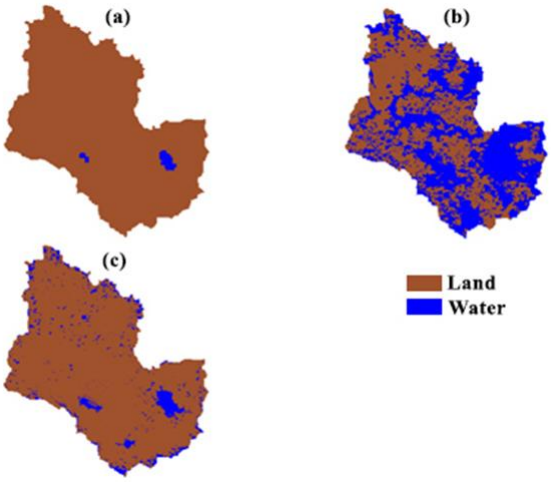

Fig. 7. Land and water classification in (a) pre-flooding, (b) flooding phase, and (c) post-flooding

CONCLUSIONS

Studia Universitatis "Vasile Goldiş", Seria Ştiinţele Vieţii
Vol. 28 issue 4, 2018, pp. 159-166

Thailand is basically under the influence of 2 types of monsoons, namely the southwest and northeast monsoons. This is why we have 2 obvious seasons, the wet and dry seasons, switching between them. For the dry season, it can be split into the 2 other seasons, i.e., summer and winter when investigating elaborately. Thailand, therefore, can divide its seasons into 3, namely, summer, rain, and winter. SONCA was the 9th seasonal tropical storm caused by Pacific typhoon in 2017. It brought about heavy rain and devastating damage to the northeastern part of Thailand. From 26 to 29 July 2017, the highest rainfall measured was 245.00 mm. in Muang Sakon Nakhon District. This study highlighted the exploration of an inundation area examination approach suitable for the regional level, particularly in the northeastern part of Thailand. The flooding in Sakon Nakhon in 2017 was taken as a case study. Data from Terra/Modis was used along with the 4 designed physical models, comprising NDVI, NDWI, MNDWI, and DFI. The findings of implementation identified that DFI exhibited the highest percentage of analysis accuracy, as previously mentioned. The findings of this study should be applied as a logical criterion for decisions about inundation areas and for rapid as well as reliable assessment. Involved agencies may count on this approach for inundation area analysis. The analysis results should then be employed to support planning for sustainable flooding prevention and relief in the future.

ACKNOWLEDGEMENTS

This Research was Financially Supported by Faculty of Science, Mahasarakham University (Grant year 2019).

REFERENCES

Amini, J. A method for generating floodplain maps using IKONOS images and DEMs. International Journal of Remote Sensing, 31(9), 2441-2456, 2010.

Asian Disaster Reduction Center. Natural Disaster Data Book. Asian Disaster Reduction Center (ADRC), 2012.

Blanc, J., Hall, J., Roche, N., Dawson, R., Cesses, Y., Burton, A., and Kilsby, C. Enhanced efficiency of pluvial flood risk estimation in urban areas using spatial–temporal rainfall simulations. Journal of Flood Risk Management, 5, 143–152, 2012.

Brunda, G.S., Nyamathi, S.J. Derivation and Analysis of Dimensionless Hydrograph and S Curve for Cumulative Watershed Area. Aquatic Procedia. 4, 964-971, 2015.

Department of Disaster Prevention and Mitigation. Ministry of Interior. Thailand. Report Analysis/Monitoring. 2013; http://www.disaster.go.th/th/ dwn-download-12-1/

Elkhrachy, I. Flash Flood Hazard Mapping Using Satellite Images and GIS Tools: A case study of Najran City, Kingdom of Saudi Arabia (KSA). The Egyptian Journal of Remote Sensing and Space Science, 18(2), 261-278, 2015.

Gao, B.C. NDWI—a normalized difference water index for remote sensing of vegetation liquid water from space. Remote Sensing of Environment, 58, 257-266, 1996.

Gates, D. M. Biophysical Ecology, Springer-Verlag, New York, 611 p, 1980.

Kia, M. B., Pirasteh, S., Pradhan, B., Mahmud, A. R., Sulaiman, W. N. A., and Moradi, A. An artificial neural network model for flood simulation using GIS: Johor River Basin, Malaysia. Environmental Earth Sciences. 67(1), 1-14, 2012.

Kim, B., Sanders, B. F., Schubert, J. E., and Famiglietti, J. S. Mesh type tradeoffs in 2D hydrodynamic modeling of flooding with a Godunov-based flow solver. Advances in Water Resources, 68, 42-61, 2014.

Krausmann E, Mushtaq F. A qualitative Natech damage scale for the impact of floods on selected industrial facilities. Natural Hazards. 46(2), 179–97, 2008.

Laosuwan, T., Uttaruk, Y. Application of Geo-informatics and Vegetation Indices to Estimate Above-ground Carbon Sequestration. Studia Universitatis Vasile Goldis Arad, Seria Stiintele Vietii, 26(4), 449-454, 2016.

McFeeters, S.K. The use of normalized difference water index (NDWI) in the delineation of open water features. International Journal of Remote Sensing, 17, 1425-1432, 1996.

Milly, P.C., Wetherald, R.T., Dunne, K.A., Delworth, T.L. Increasing Risk of Great Floods in a Changing Climate. Nature. 15(6871), 514-517, 2002.

Rotjanakusol, T., Laosuwan, T. Remote Sensing Based Drought Monitoring In The Middle-Part Of Northeast Region Of Thailand. Studia Universitatis Vasile Goldis Arad, Seria Stiintele Vietii, 28(1), 14-21, 2018.

Saini, S. S., and Kaushik, S. P. Risk and vulnerability assessment of flood hazard in part of Ghaggar Basin: A case study of Guhla block, Kaithal, Haryana, India. International Journal of Geomatics and Geosciences, 3(1), 42-54, 2012.

Singh, K.K., Singh, A. Identification of flooded area from satellite images using Hybrid Kohonen Fuzzy C-Means sigma classifier. The Egyptian Journal of Remote Sensing and Space Science. 21(1), 147-155, 2017.

Thai Meteorological Department. Meteorological Book. 2017; https://www.tmd.go.th/info/info.php?FileID=70

Uttaruk, Y., Laosuwan, T. Remote sensing based vegetation indices for estimating above ground carbon sequestration in orchards Agriculture & Forestry. 62(4), 193-201, 2016.

Uttaruk, Y., Laosuwan, T. Community Forest for Global Warming Mitigation: The Technique for Estimation of Biomass and Above Ground Carbon Storage using Remote Sensing Method. Agriculture & Forestry. 64(3), 47-57, 2018.

Wang, S. The Quantitative Research on Dynamic Changes between flood and Vegetation in

Tarim. PhD-Dissertation, Beijing Normal University, Beijing, 2007.

Xu, H. Modification of Normalized Difference Water Index (NDWI) to Enhance Open Water Features in Remotely Sensed Imagery. International Journal of Remote Sensing, 27(14), 3025-3033, 2006.